

Data-driven feedforward control design for nonlinear systems: A control-oriented system identification approach*

Max Bolderman^{†,1}, Mircea Lazar¹, and Hans Butler^{1,2}

Abstract—Feedforward controllers typically rely on accurately identified inverse models of the system dynamics to achieve high reference tracking performance. However, the impact of the (inverse) model identification error on the resulting tracking error is only analyzed a posteriori in experiments. Therefore, in this work, we develop an approach to feedforward control design that aims at minimizing the tracking error a priori. To achieve this, we show that the norm of the tracking error can be upperbounded by the sum of the inversion error and the identification error. This yields a two-step feedforward control design procedure that consists of a feedforward control-oriented system identification, and a finite-horizon optimization to compute the feedforward control signal. The nonlinear feedforward control design method is validated using physics-guided neural networks on a nonlinear, nonminimum phase mechatronic example, where it outperforms standard ILC.

I. INTRODUCTION

Feedforward control is a dominant actor in achieving high reference tracking performance within high-precision mechatronic industries. The achieved performance is typically limited by the accuracy of the model describing the dynamics as well as the accuracy of the inversion [1]. Conventional feedforward controllers derived from linear models are therefore intrinsically limited. Indeed, linear models are not capable to describe the complete dynamical behaviour of a mechatronic system, which includes unknown dynamics arising from, e.g., manufacturing tolerances [2]. Consequently, there is an interest to employ rich, nonlinear models for feedforward control that can learn the unknown dynamics from data [3]. This, however, brings (new) challenges to feedforward control design, which are briefly discussed next.

A common approach to feedforward control design is inverse model-based feedforward, which generates the feedforward signal by passing the reference through a model of the inverse system dynamics, see, e.g., [4], [5]. When the model of the system is nonminimum phase, i.e., it has an unstable inverse, different methods are available to generate a stable feedforward controller, see, e.g., [5], [6]. These methods however, are not directly extendable to nonlinear feedforward controllers. Hence, a different approach is to formulate feedforward control as an optimization problem, where the goal is to minimize the norm of the difference between the reference and the model output. Within this category, it is possible to optimize the complete feedforward

signal [7], [8], or to parameterize the feedforward signal as a function of time or the reference and optimize over the parameters [9], [10]. When the system performs a repetitive task, an iterative learning control (ILC) method can be used to minimize the tracking error based on the tracking error of previous repetitions by updating the feedforward input [11], the parameters of an inverse model [12], or both [13].

The aforementioned methods typically assume a known, physics-based model of the system. To account for unknown or complex to model dynamics, data-driven techniques have been explored in combination with artificial intelligence, e.g., neural network (NN) models [14], physics-informed neural networks [15], or physics-guided neural network (PGNN) models [16] and other hybrid model structures [17]. However, due to the non-invertibility of (PG)NN models, these approaches generally adopt an identification of the inverse system directly. Thereby, the objective function minimized during the identification is not related to the reference tracking objective. In [18], a control-relevant identification cost function, which filters the inverse model error with a linear model of the process sensitivity was proposed to mitigate this issue. To the best of the authors' knowledge, a framework for feedforward control design for nonlinear systems that quantifies the relation between the identification error and the resulting tracking error is not yet available.

Motivated by the above observations, in this paper we develop a nonlinear data-driven feedforward control design method that aims to minimize the tracking error a priori. To achieve this, we derive a fundamental upperbound on the norm of the tracking error in terms of the norm of the identification error, i.e., how well is the system identified, and the inversion error, i.e., how well is the feedforward control input designed for the identified model. This is in the spirit of [19], which merges the identification and feedback control design in a single framework for linear systems. To minimize the tracking error, we develop a two-step procedure:

- 1) *Indirect closed-loop identification* based on a data set which should include relevant operating conditions;
- 2) *Feedforward control input design* by minimizing the norm of the difference between the reference and the predicted output of the identified model.

We formulate a finite horizon optimal feedforward control (FHOFC) problem to design the feedforward input. Similar formulations were used in [8] and [7] for linear and nonlinear systems, respectively. Several directions are highlighted to reduce the computational complexity induced by optimizing the complete feedforward signal. Generality of the devel-

*This work is supported by the NWO research project PGN Mechatronics, project number 17973.

[†]Corresponding author: m.bolderman@tue.nl.

¹Control Systems Group, Eindhoven University of Technology, Groene Loper 19, Eindhoven, 5612 AP, The Netherlands.

²ASML, De Run 6501, Veldhoven, 5504 DR, The Netherlands.

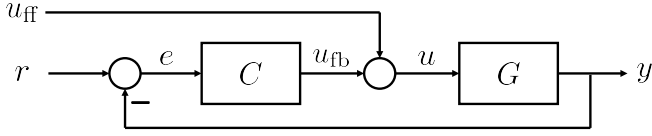


Fig. 1. Schematic overview of the control structure.

oped FHOFC formulation is demonstrated by recovering inverse model-based feedforward and linear ILC for specific settings. The FHOFC is directly applicable to nonlinear, multi-input multi-output (MIMO) systems, which can be nonminimum phase and in state-space representation, while it allows for specifying constraints on the inputs, outputs, and states.

II. PRELIMINARIES

We consider the feedforward control design for a system G operating in closed-loop with feedback controller C as visualized in Fig. 1. Let $k \in \mathbb{Z}_{\geq 0}$ be the discrete time instant. Then, $y(k) \in \mathbb{R}^{n_y}$ is the output at time k , $r(k) \in \mathbb{R}^{n_y}$ the reference, $e(k) := r(k) - y(k)$ the tracking error, and $u(k) \in \mathbb{R}^{n_u}$ the input with $n_y, n_u \in \mathbb{Z}_{>0}$ the number of outputs and inputs, respectively. The input $u(k)$ is the sum of the feedback and feedforward inputs, such that $u(k) := u_{fb}(k) + u_{ff}(k)$. We assume that a stabilizing feedback controller is available, e.g., it is tuned from a frequency response function. We denote a signal of length $N_k \in \mathbb{Z}_{>0}$ by its capital symbol letter, e.g.,

$$Y := [y^T(0), \dots, y^T(N_k - 1)]^T. \quad (1)$$

When supplied with a reference and feedforward input, the closed-loop system generates an output satisfying

$$Y = \Phi(x_0, R, U_{ff}), \quad (2)$$

where $x_0 \in \mathbb{R}^{n_x}$ is the initial state, and $\Phi : \mathbb{R}^{n_x} \times \mathbb{R}^{N_k n_y} \times \mathbb{R}^{N_k n_u} \rightarrow \mathbb{R}^{N_k n_y}$ is a (partially) unknown mapping that specifies Y in terms of x_0 , R , and U_{ff} . For an x_0 of interest, a data set of length $N_d \in \mathbb{Z}_{>0}$ is generated on the system, such that we have Y^d , R^d , and U_{ff}^d satisfying (2), i.e.,

$$Y^d = \Phi(x_0, R^d, U_{ff}^d). \quad (3)$$

Remark 2.1: The user can freely design R^d and U_{ff}^d supplied during the data generation experiment. Typically, R^d is chosen to include the references for which we aim to find a feedforward input, while U_{ff}^d serves as an excitation signal.

The optimal feedforward control input U_{ff} minimizes the tracking error $E = R - Y$ according to a chosen norm, i.e.,

$$U_{ff} = \arg \min_{U_{ff}} \|R - Y\|. \quad (4)$$

The mapping Φ in (2) is unknown, which means that the output Y in (4) cannot be computed as a function of the feedforward input U_{ff} , i.e., Y can only be generated by fixing U_{ff} and performing an experiment on the system. Therefore, it is common to parameterize a model of Φ , such that

$$\hat{Y} = \hat{\Phi}(\theta, x_0, R, U_{ff}), \quad (5)$$

where \hat{Y} is a prediction of the output Y , $\hat{\Phi} : \mathbb{R}^{n_\theta} \times \mathbb{R}^{n_x} \times \mathbb{R}^{N_k n_y} \times \mathbb{R}^{N_k n_u} \rightarrow \mathbb{R}^{N_k n_y}$ a parameterized model of Φ , and $\theta \in \mathbb{R}^{n_\theta}$ the model parameters with $n_\theta \in \mathbb{Z}_{>0}$. The mapping in (5) can be obtained by simulation of a model of the system dynamics, which can be input-output

$$\hat{y}(k) = f(\theta, [\hat{y}^T(k-1), \dots, \hat{y}^T(k-n_a), \hat{u}^T(k-n_k-1), \dots, \hat{u}^T(k-n_k-n_b)]^T), \quad (6)$$

or state-space

$$\begin{aligned} \hat{x}(k+1) &= f_x(\theta, \hat{x}(k), \hat{u}(k)), \\ \hat{y}(k) &= g_x(\theta, \hat{x}(k)), \end{aligned} \quad (7)$$

operating in closed-loop with, e.g., a linear output feedback

$$\hat{u}(k) = C(q)(r(k) - \hat{y}(k)) + u_{ff}(k). \quad (8)$$

Remark 2.2: A suitable model class for nonlinear feedforward control, which is used in this paper, are PGNNs [16]. For example, for a single-input single-output (SISO) system, i.e., $n_y = n_u = 1$, the PGNN in input-output form (6) is given as

$$\begin{aligned} \hat{y}(k) &= f_{\text{phy}}(\theta_{\text{phy}}, \phi(k)) + f_{\text{NN}}(\theta_{\text{NN}}, \phi(k)), \\ \phi(k) &= [\hat{y}(k-1), \dots, \hat{y}(k-n_a), \\ &\quad \hat{u}(k-n_k-1), \dots, \hat{u}(k-n_k-n_b)]^T, \end{aligned} \quad (9)$$

where $n_a, n_b, n_k \in \mathbb{Z}_{\geq 0}$ describe the order of the dynamics, $f_{\text{phy}} : \mathbb{R}^{n_{\text{phy}}} \times \mathbb{R}^{n_a+n_b} \rightarrow \mathbb{R}$ is a known model derived from physics, $f_{\text{NN}} : \mathbb{R}^{n_{\text{NN}}} \times \mathbb{R}^{n_a+n_b} \rightarrow \mathbb{R}$ is a neural network, and $\theta = [\theta_{\text{phy}}^T, \theta_{\text{NN}}^T]^T$ are the parameters.

III. PROBLEM FORMULATION

Since the mapping Φ in (2) is unknown, the feedforward control design is based on a model-based mapping $\hat{\Phi}$ as in (5). This typically yields a two-step feedforward controller design procedure, consisting of an *identification* step to fit the model (5) to the data (3), and an *inversion* step to compute the feedforward input. Although this approach is generally adopted in literature, see, e.g., [3], [15], [16], [18], a quantitative relation between the identification and the tracking error, respectively, is still missing. Hence, the first problem considered in this work is to establish a quantitative relation between the tracking error on one hand, and the identification error and inversion error on the other hand.

The identification step typically finds the parameters $\theta = \hat{\theta}$ for the model (5) by minimizing a cost function, such that

$$\hat{\theta} = \arg \min_{\theta} V(\theta, Y^d, R^d, U_{ff}^d). \quad (10)$$

Therefore, the second problem considered is how to choose the cost function $V(\theta, Y^d, R^d, U_{ff}^d)$ such that the identified parameters $\hat{\theta}$ yield a model-based mapping $\hat{\Phi}(\hat{\theta}, x_0, R, U_{ff})$ that is suitable for the design of a feedforward controller.

Often, the nonlinear inverse model-based feedforward controller suffers a performance loss when the forward model is nonminimum phase. For example, [3] imposes stability of PGNN feedforward controllers by constraining the NN parameters based on sufficient conditions for stability. This might unnecessarily limit the flexibility of the PGNN model,

and, consequently, the accuracy of the identification. Hence, it would be of interest to develop a general nonlinear feedforward control framework for the identified model-based mapping $\hat{\Phi}(\hat{\theta}, x_0, R, U_{\text{ff}})$ which is capable to deal with nonlinear, nonminimum phase MIMO systems, state-space representations, and constraints on the inputs, outputs, or states.

In what follows, we derive an explicit upperbound on the reference tracking performance for any feedforward control signal, which opens the path to such a generally applicable data-driven feedforward control design method.

IV. FEEDFORWARD CONTROL-ORIENTED IDENTIFICATION

To derive the bound on the tracking error, we define the inversion error as $R - \hat{\Phi}(\theta, x_0, R, U_{\text{ff}})$ and the model error as $Y - \hat{\Phi}(\theta, x_0, R, U_{\text{ff}})$.

Proposition 4.1: Consider the mapping (2) and a corresponding parameterized model-based mapping (5). Then, for any θ and U_{ff} , the norm of the corresponding tracking error is upperbounded by the sum of the norms of the inversion and model error, respectively, i.e.,

$$\|R - Y\| \leq \|R - \hat{\Phi}(\theta, x_0, R, U_{\text{ff}})\| + \|Y - \hat{\Phi}(\theta, x_0, R, U_{\text{ff}})\|. \quad (11)$$

Proof: The proof follows by applying the triangle inequality, such that

$$\begin{aligned} \|R - Y\| &= \|R - \hat{Y} + \hat{Y} - Y\| \\ &\leq \|R - \hat{Y}\| + \|\hat{Y} - Y\| = \|R - \hat{Y}\| + \|Y - \hat{Y}\|. \end{aligned} \quad (12)$$

Eq. (11) is obtained by substituting (5) in (12). \blacksquare

Proposition 4.1 states that the norm of the tracking error can be decreased by minimizing the norm of the inversion and the model error, respectively. Computation of the model error requires Y , which can only be generated on the system by applying U_{ff} , which is yet unknown. Therefore, we replace the model error by the identification error, i.e.,

$$Y^d - \hat{\Phi}(\theta, x_0, R^d, U_{\text{ff}}^d). \quad (13)$$

The identification error (13) can be made smaller by appropriately choosing θ . Thereby, we obtain a two-step approach to design a data-driven nonlinear feedforward controller:

- 1) **Identify** the set of parameters $\theta = \hat{\theta}$ that minimizes the norm of the identification error, such that $\hat{\theta} = \arg \min_{\theta} \|Y^d - \hat{\Phi}(\theta, x_0, R^d, U_{\text{ff}}^d)\|$;
- 2) **Compute** the feedforward input U_{ff} that minimizes the norm of the inversion error for $\theta = \hat{\theta}$, such that $U_{\text{ff}} = \arg \min_{U_{\text{ff}}} \|R - \hat{\Phi}(\hat{\theta}, x_0, R, U_{\text{ff}})\|$.

Step 1) shows that the cost function V in (10) should be chosen as the norm of the *closed-loop simulation error*.

Lemma 4.1: Consider the mapping (2) and the parameterized model-based mapping (5), where $\hat{\theta}$ and U_{ff} are found by the two-step approach above. Suppose that the p -norm is used, $p \in \mathbb{Z}_{>0}$, and define the data informativity measure

$$\varepsilon := \frac{1}{N_k^{1/p}} \|Y - \hat{Y}\|_p - \frac{1}{N_d^{1/p}} \|Y^d - \hat{Y}^d\|_p. \quad (14)$$

Then, the tracking error satisfies the following bound

$$\begin{aligned} \frac{1}{N_k^{1/p}} \|R - Y\|_p &\leq \frac{1}{N_k^{1/p}} \|R - \hat{\Phi}(\hat{\theta}, x_0, R, U_{\text{ff}})\|_p \\ &\quad + \frac{1}{N_d^{1/p}} \|Y^d - \hat{\Phi}(\hat{\theta}, x_0, R^d, U_{\text{ff}}^d)\|_p + \varepsilon. \end{aligned} \quad (15)$$

Proof: Dividing both sides in (11) by $N_k^{1/p}$ and substituting (14) yields (15). \blacksquare

The division with $N_k^{1/p}$ normalizes the difference in length of Y and Y^d , i.e., when $N_k \neq N_d$. The parameter ε in (14) is a data informativity measure stating the relevance of the training data $\{Y^d, R^d, U_{\text{ff}}^d\}$ with respect to the operation data $\{Y, R, U_{\text{ff}}\}$ for the identified set of parameters $\hat{\theta}$.

Remark 4.1: From the definition (14) we have that $\varepsilon = 0$ when $\{Y^d, R^d, U_{\text{ff}}^d\} = \{Y, R, U_{\text{ff}}\}$. This hints to choosing R^d and U_{ff}^d in the data generating experiment close to R and U_{ff} to achieve a small ε , see also [20]. A reasonable choice is to have R^d comprise of a set of target references, while U_{ff}^d is generated using a simple feedforward controller. Iterative identification using data generated with a new U_{ff}^d potentially decreases ε , see also [19] for iterative linear identification and feedback controller design.

Remark 4.2: In the (PG)NN-based feedforward control literature it is common to employ a regularization term in the cost function [3, Section 4] and to use the squared 2-norm due to its smoothness, such that

$$\hat{\theta} = \arg \min_{\theta} \|Y^d - \hat{\Phi}(\theta, x_0, R^d, U_{\text{ff}}^d)\|_2^2 + \|\Lambda(\theta - \theta^*)\|_2^2. \quad (16)$$

In (16), θ^* is a set of desired parameters, e.g., 0 for θ_{NN} and/or some known physical values for θ_{phy} , and $\Lambda \in \mathbb{R}^{n_{\theta} \times n_{\theta}}$ states the relative importance of $\theta - \theta^*$. Since the norm is non-negative and the square root is monotonically increasing, minimization of the norm and its square is equivalent (when neglecting the regularization term). Hence, (16) is a suitable identification cost function when aiming to minimize the 2-norm of the tracking error, i.e., $\|R - Y\|_2$.

Remark 4.3: A similar derivation as presented in this section can be performed for a *direct* closed-loop identification. This approach has the potential for consistent identification when noise is present in the data set, see, e.g., [21].

V. FINITE-HORIZON OPTIMAL FEEDFORWARD CONTROL

Based on Lemma 4.1 we formulate the FHOFC problem as follows:

$$\begin{aligned} U_{\text{ff}} &= \arg \min_{U_{\text{ff}}} \|R - \hat{\Phi}(\hat{\theta}, x_0, R, U_{\text{ff}})\| + \|\Gamma U_{\text{ff}}\|, \\ \text{subject to: } &U_{\text{ff}} \in \mathcal{R}_{U_{\text{ff}}}, \hat{U} \in \mathcal{R}_U, \hat{Y} \in \mathcal{R}_Y, \hat{X} \in \mathcal{R}_X. \end{aligned} \quad (17)$$

In (17), $\|\Gamma U_{\text{ff}}\|$ is a regularization term used to, e.g., penalize energy consumption or changes in the feedforward signal. Additionally, $\mathcal{R}_{U_{\text{ff}}}$, \mathcal{R}_U , \mathcal{R}_Y and \mathcal{R}_X are the admissible sets of the feedforward and overall control inputs, outputs and states, respectively. Note that, \hat{U} , \hat{Y} and \hat{X} are used since U , Y and X are unknown when designing the feedforward signal. Since $\hat{U} \approx U$, $\hat{Y} \approx Y$ and $\hat{X} \approx X$, the constraints

for the real trajectories may be violated. Still, this is an improvement to unconstrained feedforward control design.

Remark 5.1: The FHOFC problem (17) can be solved for any reference and, therefore, is task flexible. Changes in the feedback controller are directly implementable in $\hat{\Phi}$.

It is worth to mention that solving (17) becomes computationally expensive when N_k is large. A constrained Gauss–Newton approach was proposed in [7] to solve the optimization by explicitly using the partial derivatives of the norm with respect to the feedforward inputs. Several other options to reduce the computational complexity are:

- 1) *Parameterize the feedforward signal* using basis functions [9], [22]. Essentially, choose $U_{\text{ff}} = \sum_{i=1}^{N_{\text{bf}}} c_i \Psi_i$ with c_i the coefficients, Ψ_i the basis functions, $N_{\text{bf}} \ll N_k$, and optimize over $c = [c_1, \dots, c_{N_{\text{bf}}}]^T$.
- 2) *Parameterize an inverse model* as $U_{\text{ff}} = \hat{\Phi}_{\text{inv}}(\theta_{\text{inv}}, R)$ and find $\hat{\theta}_{\text{inv}}$ by minimizing (17).
- 3) *Solve the FHOFC problem in a receding horizon manner*, i.e., let $\bar{u}_{\text{ff}}(k) = [u_{\text{ff}}^T(k), \dots, u_{\text{ff}}^T(k+h)]^T$, with $h \in \mathbb{Z}_{>0}$ the prediction horizon and solve

$$\bar{u}_{\text{ff}}(k) = \arg \min_{\bar{u}_{\text{ff}}(k)} \|\bar{r}(k) - \hat{y}(k)\| + \|\Gamma \bar{u}_{\text{ff}}(k)\|, \quad (18)$$

$$u_{\text{ff}}(k) = [I, 0, \dots, 0] \bar{u}_{\text{ff}}(k).$$

Next we show that the FHOFC design procedure for nonlinear systems can recover some of the state-of-the-art methods for feedforward control, namely: inverse model-based feedforward and linear ILC. To show the former, let the system model admit an input–output representation (6), and suppose that a unique inverse relation is known, such that, with a slight abuse of notation, we have

$$\hat{u}(k) = f^{-1}(\theta, [\hat{y}^T(k+n_k+1), \dots, \hat{y}^T(k+n_k-n_a+1), \hat{u}^T(k-1), \dots, \hat{u}^T(k-n_b+1)]^T). \quad (19)$$

Lemma 5.1: Consider the feedforward control design using an identified input–output model (6) for which the inverse relation (19) is unique. Suppose that the initial conditions are such that $y(i) = r(i)$ for $i \in \{k-n_a+1, \dots, n_k\}$. Then, the inverse model-based feedforward controller

$$u_{\text{ff}}(k) = f^{-1}(\hat{\theta}, [r^T(k+n_k+1), \dots, r^T(k+n_k-n_a+1), u_{\text{ff}}^T(k-1), \dots, u_{\text{ff}}^T(k-n_b+1)]^T) \quad (20)$$

solves the unconstrained receding horizon FHOFCP (18) with $\Gamma = 0$ and $h = n_k + 1$.

Proof: $u_{\text{ff}}(k)$ appears first in the predicted output $\hat{y}(k+n_k+1)$, such that $u_{\text{ff}}(k+i)$, $i \in \mathbb{Z}_{>0}$ does not play a role in the cost function when $\Gamma = 0$. Hence, the receding horizon FHOFC (18) with no constraints becomes

$$u_{\text{ff}}(k) = \arg \min_{u_{\text{ff}}(k)} \|r(k+n_k+1) - \hat{y}(k+n_k+1)\|. \quad (21)$$

Since the minimum is attained for $r(k+n_k+1) = \hat{y}(k+n_k+1)$, the solution of (21) equals (20) when (21) is solved sequentially, i.e., for $k = 0, 1, \dots, N_k$. Observing that, from (8), $u_{\text{fb}}(k) = 0$ for $r(i) - \hat{y}(i) = 0$, $i \in \{0, \dots, k\}$, such that $\hat{u}(k) = u_{\text{ff}}(k)$ completes the proof. ■

Remark 5.2: In general, obtaining an analytical inverse relation as in (19) is not possible or tractable, e.g., when the system model (6) is parametrized as a black–box NN. In these cases, $u_{\text{ff}}(k)$ can be found by minimizing (21) using a numerical solver, as in [21].

Even when the identification in (16) and the FHOFC problem (17) are solved accurately, it is still possible that the tracking error remains too large due to the presence of ε in (15). Options to generate new data and thereby achieve a smaller ε were indicated in Sec. IV. Alternatively, it is possible to use an iterative learning scheme when the same reference is executed repetitively, as done in ILC [11].

Next, we present an iterative learning FHOFC (IL–FHOFC) scheme for nonlinear systems, inspired by ILC:

$$\begin{aligned} R^{(i+1)} &= \hat{Y}^{(i)} + \alpha E^{(i)}, \\ U_{\text{ff}}^{(i+1)} &= \arg \min_{U_{\text{ff}}} \|R^{(i+1)} - \hat{\Phi}(\hat{\theta}, x_0, R, U_{\text{ff}})\| + \|\Gamma u_{\text{ff}}\|, \end{aligned} \quad (22)$$

where the superscript (i) denotes the iteration index for signals, $i \in \mathbb{Z}_{>0}$, and $E := [e^T(0), \dots, e^T(N_k - 1)]^T$. The following result shows that (22) recovers the standard ILC solution in the linear case.

Lemma 5.2: Suppose that G is the transfer function matrix of a linear system, C is a feedback controller, and \hat{G} is a model of G , with all transfer functions represented in the digital domain. Let $\hat{\Phi}$ be the closed–loop model-based mapping obtained from C and \hat{G} , and let $\alpha \in (0, 1]$ be a learning gain. Then, the ILC update law

$$u_{\text{ff}}^{(i+1)}(k) = u_{\text{ff}}^{(i)}(k) + \alpha \hat{G}^{-1}(1 + \hat{G}C)e^{(i)}(k), \quad (23)$$

solves the IL–FHOFC problem (22) with $\Gamma = 0$.

Proof: The output predicted by \hat{G} at iteration i is

$$\hat{y}^{(i)}(k) = (1 + \hat{G}C)^{-1} \hat{G}C r(k) + (1 + \hat{G}C)^{-1} \hat{G} u_{\text{ff}}^{(i)}(k). \quad (24)$$

Substituting the ILC update law (23) in (24) gives

$$\hat{y}^{(i+1)}(k) = \hat{y}^{(i)}(k) + \alpha e^{(i)}(k). \quad (25)$$

Placing the time entries of (25) in a column, shows that

$$\begin{aligned} \|R^{(i+1)} - \hat{\Phi}(\hat{\theta}, x_0, R, U_{\text{ff}}^{(i+1)})\| \\ = \|R^{(i+1)} - \hat{Y}^{(i)} - \alpha E^{(i)}\| = 0. \end{aligned} \quad (26)$$

Non-negativeness of the norm implies that (23) is a global optimum of (22) when $\Gamma = 0$. ■

Remark 5.3: An alternative approach is to re-identify θ based on new data, and compute $U_{\text{ff}}^{(i+1)}$ by using the FHOFC (17), see [23].

Remark 5.4: The update of $R^{(i)}$ in (22) is based on $\hat{Y}^{(i-1)}$ since the optimization does not necessarily yield $R^{(i)} = \hat{Y}^{(i)}$.

VI. VALIDATION ON A NONMINIMUM PHASE NONLINEAR MECHATRONIC EXAMPLE

System description: We consider the position control of a translating–rotating mass with force input u and position

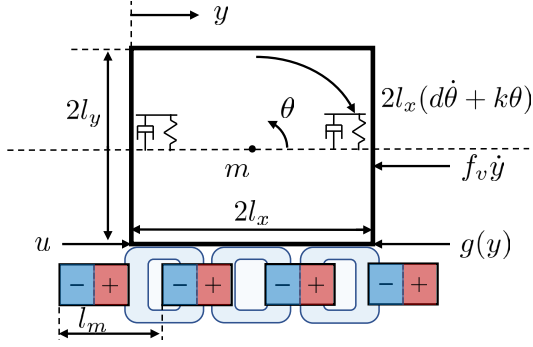


Fig. 2. Rotating–translating mass with actuation and sensing on opposite sides of the centre of mass.

TABLE I

PARAMETER VALUES OF THE SYSTEM DISPLAYED IN FIG. 2.

m	l_x, l_y	J	f_v	k	d	l_m	c
20	1	$\frac{40}{3}$	50	$\frac{25 \cdot 10^3}{3}$	$\frac{575}{3}$	0.05	1
kg	m	kgm^2	$\frac{kg}{s}$	$\frac{kg}{s^2}$	$\frac{kg}{s}$	m	N

output y at opposite sides of the centre of mass, see Fig. 1 and [3]. The continuous–time dynamics is given as

$$\begin{aligned}
 Jm \frac{d^4 y}{dt^4} + (f_v J + 2l_x dm) \frac{d^3 y}{dt^3} \\
 + 2(l_x df_v + l_x km) \frac{d^2 y}{dt^2} + 2l_x k f_v \frac{dy}{dt} \\
 = (J - l_y^2 m) \frac{d^2 \xi}{dt^2} + (2l_x d - l_y^2 f_v) \frac{d\xi}{dt} + 2l_x k \xi.
 \end{aligned} \quad (27)$$

In (27), $l_x, l_y \in \mathbb{R}_{\geq 0}$ are the width and height of the mass $m \in \mathbb{R}_{> 0}$, $J = \frac{1}{3}(l_x^2 + l_y^2)$ is the moment of inertia, $f_v \in \mathbb{R}_{> 0}$ the viscous friction coefficient, and $d, k \in \mathbb{R}_{> 0}$ the damping and spring constant counteracting the rotation from both ends of the mass. The auxiliary input ξ is given as

$$\xi := u - c \sin\left(\frac{2\pi}{l_m} y\right), \quad (28)$$

where u is the input, and the sin–function represents the cogging force which is assumed *unknown* with $l_m \in \mathbb{R}_{> 0}$ the magnet pole pitch and $c \in \mathbb{R}_{> 0}$ the cogging magnitude. Parameter values are listed in Table I. The system (27) is controlled in closed–loop at a frequency $F_s = 100$ Hz by the ZOH discretization of

$$C(s) = 5 \cdot 10^3 \frac{s + 4\pi}{s + 20\pi}. \quad (29)$$

A normally distributed noise $v(k) \sim \mathcal{N}(0, (10^{-6})^2)$ m is added as *measurement noise*, such that both the data set and the feedback controller use $y(k) + v(k)$ rather than $y(k)$.

The system (27) exhibits the following challenges for feedforward control:

- 1) *Nonlinear dynamics* in the form of a cogging force, which is assumed unknown;
- 2) *Nonminimum phase dynamics* which require non-causal actuation to return a stable feedforward signal.

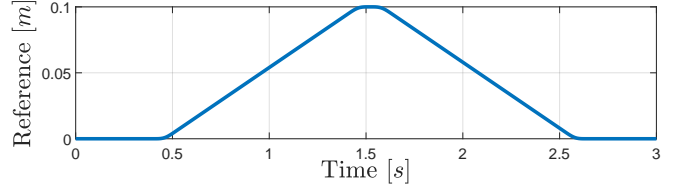


Fig. 3. Reference R used for performance evaluation.

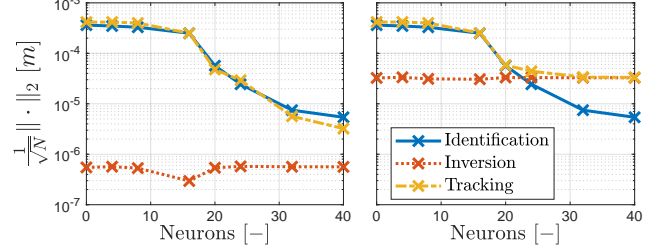


Fig. 4. Normalized 2–norm of the identification ($Y^d - \hat{Y}^d$, $N = N_d$), inversion ($R - \hat{Y}$, $N = N_k$) and tracking ($R - Y$, $N = N_k$) error for PGNNs with different number of neurons using $\gamma = 10^{-6}$ (left window) and $\gamma = 5 \cdot 10^{-5}$ (right window).

Data generation: The training data is generated in closed–loop by sampling the output $y^d(k)$ at the frequency F_s for a duration of 45 s. The reference R^d is a concatenation of 15 times the third order reference R in Fig. 3, which has bounded velocity $|\frac{d}{dt} r^d| \leq 0.1 \frac{m}{s}$, acceleration $|\frac{d^2}{dt^2} r^d| \leq 4 \frac{m}{s^2}$ and jerk $|\frac{d^3}{dt^3} r^d| \leq 40 \frac{m}{s^3}$. Additionally, U_{ff}^d is a zero–mean white noise with variance $\sigma^2 = 20^2 N^2$ for $t = [10, 40]$ s.

Model parameterization: We parameterize the system with an input–output PGNN model (9) as proposed in [16], with a *linear physical model* and a *black–box NN* with one hidden layer with n_1 neurons using tanh activation, i.e.,

$$\hat{y}(k) = \theta_{\text{phy}}^T \phi(k) + W_2 \tanh(W_1 \phi(k) + B_1) + B_2. \quad (30)$$

In (30), $\theta_{\text{NN}} = [\text{col}(W_1)^T, B_1^T, \text{col}(W_2)^T, B_2^T]^T$, where $\text{col}(W_i)$ stacks the columns of W_i . ZOH discretization of the linear part of (27) gives $n_a = n_b = 4$, $n_k = 0$ in $\phi(k)$.

System identification: The PGNN parameters are identified according to (16) (using the *lsqnonlin* MATLAB function) with $\Lambda = [I, 0]$, $\theta^* = [\theta_{\text{phy}}^*, 0]^T$, and θ_{phy}^* the parameters identified with the physical model.

Feedforward: The feedforward signals U_{ff} have length $N_k = 300$ and are computed by solving the FHOFC (17) while penalizing the rate of change in U_{ff} by choosing

$$\Gamma = \gamma \Delta, \quad (31)$$

where $\gamma \in \mathbb{R}_{> 0}$ states the importance of the regularization and $\Delta \in \mathbb{R}^{N_k \times N_k}$ has 1 on the diagonal, -1 on the sub-diagonal and 0 elsewhere. Solving the FHOFC (17) converges in 7 s with *lsqnonlin* on a 2.59 GHz Intel Core–i7–9750H using MATLAB 2019A.

Results: Fig. 4 visualizes the 2–norm of the identification, inversion and tracking error in (15) for the reference R in Fig. 3 using different number of neurons n_1 , with $\gamma = 10^{-6}$ (top window) and $\gamma = 5 \cdot 10^{-5}$ (bottom window).

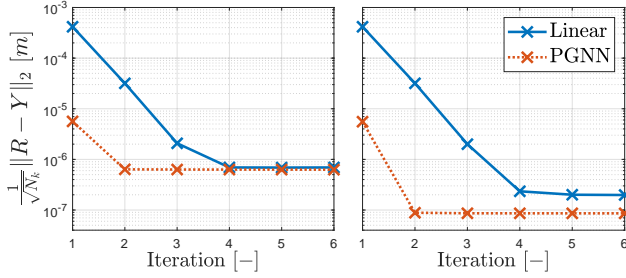


Fig. 5. Normalized 2-norm of the tracking error over the iterations using IL-FHOFC (22) with $\alpha = 1$ and $\gamma = 10^{-8}$ using a linear and a PGNN (30) model with $n_1 = 32$, simulated with $v(k) \sim \mathcal{N}(0, (10^{-6})^2)$ (left window) and with $v(k) = 0$ (right window).

Due to the nonlinearity present in the system (27), the identification error becomes smaller when increasing the number of neurons n_1 . For $\gamma = 10^{-6}$ the inversion error is small, such that the tracking error is limited by the accuracy of the identification. In contrast, for $\gamma = 5 \cdot 10^{-5}$ the inversion error increases, which limits the achievable performance for $n_i > 20$. Comparing the upperbound (15) with the results in Fig. 4 indicates that ε is small. Correspondingly, Lemma 4.1 can be used to aim for a desired reference tracking performance a priori by performing the identification and inversion sufficiently accurate.

Fig. 5 shows the 2-norm of the tracking error for a linear and a PGNN model over multiple iterations of the reference R in Fig. 3 when using the IL-FHOFC (22) with $\alpha = 1$ and $\gamma = 10^{-8}$. Since both approaches reach the noise-floor, results are added where $v(k) = 0$ to emphasize the benefit of the nonlinear PGNN model structure. The tracking error converges both faster, and to a lower value when using the PGNN model. After 6 repetitions the normalized 2-norm of the tracking error with $v(k) = 0$ is $4.96 \cdot 10^{-9} m$ for the PGNN and $1.14 \cdot 10^{-8} m$ for the linear model, respectively.

VII. CONCLUSIONS

In this paper, we presented a generalized approach to nonlinear data-driven feedforward control design from the perspective of minimizing tracking errors. We showed that the norm of the reference tracking error is upperbounded by the sum of the inversion and the identification error, respectively. This resulted in a two-step approach to feedforward control design, consisting of a feedforward control-oriented system identification followed by a finite-horizon optimization to compute the feedforward input signal. Generality of the FHOFC formulation was demonstrated by recovering inverse model-based feedforward and linear ILC for specific settings. The developed methodology was validated using physics-guided neural networks on a nonlinear, nonminimum phase mechatronic example, where it outperformed a standard ILC method.

REFERENCES

[1] S. Devasia, “Should model-based inverse inputs be used as feedforward under plant uncertainty?” *IEEE Transactions on Automatic Control*, vol. 47, pp. 1865–1871, 2002.

[2] T. T. Nguyen, “Identification and compensation of parasitic effects in coreless linear motors,” Ph.D. dissertation, Eindhoven University of Technology, The Netherlands, 2018.

[3] M. Bolderman, H. Butler, S. Koekebakker, E. van Horsen, R. Kamidin, T. Spaan-Burke, N. Strijbosch, and M. Lazar, “Physics-guided neural networks for feedforward control with input-to-state stability guarantees,” *arXiv:2301.08568*, 2023.

[4] M. L. G. Boerlage, M. Steinbuch, P. F. Lambrechts, and M. M. J. van de Wal, “Model-based feedforward for motion systems,” *IEEE International Conference on Control Applications*, vol. 2, pp. 1158–1163, 2003.

[5] J. A. Butterworth, L. Y. Pao, and D. Y. Abramovitch, “Analysis and comparison of three discrete-time feedforward model-inverse control techniques for nonminimum-phase systems,” *Mechatronics*, vol. 22, no. 5, pp. 577–587, 2012.

[6] J. van Zundert and T. Oomen, “On inversion-based approaches for feedforward and ILC,” *Mechatronics*, vol. 50, pp. 282–291, 2018.

[7] M. Volckaert, A. van Mulders, J. Schoukens, M. Diehl, and J. Swevers, “Model based nonlinear iterative learning control: A constrained gauss-newton approach,” *Mediterranean Conference on Control and Automation*, pp. 718–723, 2009.

[8] D. S. Carrasco and G. C. Goodwin, “Feedforward model predictive control,” *Annual Review in Control*, vol. 35, pp. 199–206, 2011.

[9] K. S. Ramani, M. Duan, C. E. Okwudire, and A. G. Ulsoy, “Tracking control of linear time-invariant nonminimum phase systems using filtered basis functions,” *Journal of Dynamic Systems, Measurement, and Control*, vol. 139, p. 011001, 2017.

[10] Y. Kasemsinsup, “Feedforward control for parameter-varying systems,” Ph.D. dissertation, Eindhoven University of Technology, The Netherlands, 2021.

[11] D. A. Bristow, M. Tharayil, and A. G. Alleyne, “A survey of iterative learning control,” *IEEE Control Systems Magazine*, vol. 26, no. 3, pp. 96–114, 2006.

[12] L. Blanken, F. Boeren, D. Bruijnen, and T. Oomen, “Batch-to-batch rational feedforward control: From iterative learning to identification approaches, with application to a wafer stage,” *IEEE/ASME Transactions on Mechatronics*, vol. 22, no. 2, pp. 826–837, 2017.

[13] M. B. Saltik, B. Jayawardhana, and A. Cherukuri, “Iterative learning and model predictive control for repetitive nonlinear systems via koopman operator approximation,” *IEEE Conference on Decision and Control*, pp. 3059–3065, 2022.

[14] O. Sørensen, “Additive feedforward control with neural networks,” *IFAC Proceedings Volumes*, vol. 32, no. 2, pp. 1378–1383, 1999.

[15] M. Bolderman, D. Fan, M. Lazar, and H. Butler, “Generalized feedforward control using physics-informed neural networks,” *IFAC-PapersOnline*, vol. 55, pp. 148–153, 2022.

[16] M. Bolderman, M. Lazar, and H. Butler, “Physics-guided neural networks for inversion-based feedforward control applied to linear motors,” *IEEE Conference on Control Technology and Applications*, pp. 1115–1120, 2021.

[17] C.-H. Chou, M. Dua, and C. E. Okwudire, “A physics-guided data-driven feedforward tracking controller for systems with unmodeled dynamics—applied to 3d printing,” *IEEE Access*, vol. 11, pp. 14563–14574, 2023.

[18] L. Aarnoudse, W. Ohnishi, M. Poot, P. Tacx, N. Strijbosch, and T. Oomen, “Control-relevant neural networks for intelligent motion feedforward,” *IEEE International Conference on Mechatronics*, 2021.

[19] P. M. J. van den Hof and R. J. P. Schrama, “Identification and control – closed-loop issues,” *Automatica*, vol. 31, no. 12, pp. 1751–1770, 1995.

[20] J. Schoukens and L. Ljung, “Nonlinear system identification: a user-oriented road map,” *IEEE Control Systems*, vol. 39, no. 6, pp. 28–99, 2019.

[21] M. Bolderman, M. Lazar, and H. Butler, “Physics-guided neural networks for feedforward control: From consistent identification to feedforward controller design,” *IEEE Conference on Decision and Control*, pp. 1497–1502, 2022.

[22] R. Kasemsinsup, R. Romagnali, M. F. Heertjes, S. Weiland, and H. Butler, “Reference-tracking feedforward control design for linear dynamical systems through signal decomposition,” *American Control Conference*, pp. 2387–2382, 2017.

[23] M. Volckaert, M. Diehl, and J. Swevers, “Generalization of norm optimal ILC for nonlinear systems with constraints,” *Mechanical Systems and Signal Processing*, vol. 39, no. 1–2, pp. 280–296, 2013.